ISTITUTO NAZIONALE DI GEOFISICA E VULCANOLOGIA

Site characterization report at the seismic station IT.CPC – Coccanile, Copparo (FE)

Report di caratterizzazione di sito presso la stazione sismica IT.CPC – Coccanile, Copparo (FE)

Working Group **Geology:** Luca MINARELLI[1], Marco STEFANI[2] **Geophysics:** Giuseppe DI GIULIO[1], Giuliano MILANA[1], Maurizio VASSALLO[1] (1) Istituto Nazionale di Geofisica e Vulcanologia (2) Università degli Studi di Ferrara	Date: December 2021

Subject: **Final report illustrating the site characterization for seismic station IT.CPC**

Convenzione DPC-INGV 2019-21, All.B2- WP1, Task 2: "Caratterizzazione siti accelerometrici" (Coord.: G.Cultrera, F. Pacor)
Cite as: Working group INGV "Agreement DPC-INGV 2019-21, All.B2- WP1, Task 2", (2021). Site characterization report at the seismic station IT.CPC – Coccanile, Copparo (FE) http://hdl.handle.net/2122/15091

INDEX

INTRODUCTION

In this report we present the geological setting, and the geophysical measurements, and the results obtained in the framework of the 2019-2021 research agreement between INGV and DPC for the site characterization of station IT.CPC, called "Allegato B2: Obiettivo 1 - TASK 2: Caratterizzazione siti accelerometrici (Responsabili: G. Cultrera, F. Pacor)" .

Location and geographic coordinates are reported in Table 1.

Table 1.

CODE	NAME	LAT [°]	LON [°]	ELEVATION [m]
IT.CPC	COPPARO (COCCANILE)	44.92145*	11.87561*	1**
ADDRESS	Via Cattaneo, 63 – 44034 – Copparo (FE), Italy*			

* Reference table from ITACA – D'Amico et al., 2020 (December 2021)
** Reference Topographic basemap CTR 1:5000 - Regione Emilia-Romagna

A. Geological setting

A1. TOPOGRAPHIC AND GEOLOGICAL INFORMATION

The topographic information on the site is reported in Table 2.

Table 3 describes all the previous geological maps available for the analyses.

Table 2.

Topography	Description	Topography Class	Morphology Class	EC8 Class
	Flat top of isolated relief with slope i<=15°	T1*	P	C*

* According to the nomenclature of ITACA – D'Amico et al., 2020 (December 2021).

Table 3.

Geological map	Source	Scale
IT.CPC	Geological map of Italy sheet *N.76* (Ferrara)	1:100.000
IT.CPC	Geological and technical map – Seismic Microzonation	1:5.000

In Table 4 Geological and Lithotechnical Units used in the maps of following chapters are described (according to Seismic Microzonation classification; Technical Commission SM, 2015). The term "original" means the result comes from a preexisting cartography (Table 3); the term "deduced" means the result derives from an interpretation of a preexisting cartography, keeping its original nomenclature.

Table 4.

GEOLOGICAL UNITS		**LITHOTECHNICAL UNITS**	
Geological map - Deduced. According to the nomenclature of the geological map of Italy 1:50.000 (Sheet 187 – Codigoro)		Lithotechnical Map - Deduced. According to the nomenclature of the Seismic Microzonation (Technical Commission SM, 2015).	
code	**description**	**code**	**description**
AES8	Clays and silty clays of delta plain (Holocene)	CLdl	Medium to low plasticity inorganic clays and silty clays of delta plain
AES8	Silty sand and clayey silt of delta channel (Holocene)	MLes	Inorganic silt, silty or clayey fine sand and low-plasticity clayey silt of delta channel

A2. GEOLOGICAL MAP

In Figure 1, the Geological Map describes a 1km x 1km square area around the station.

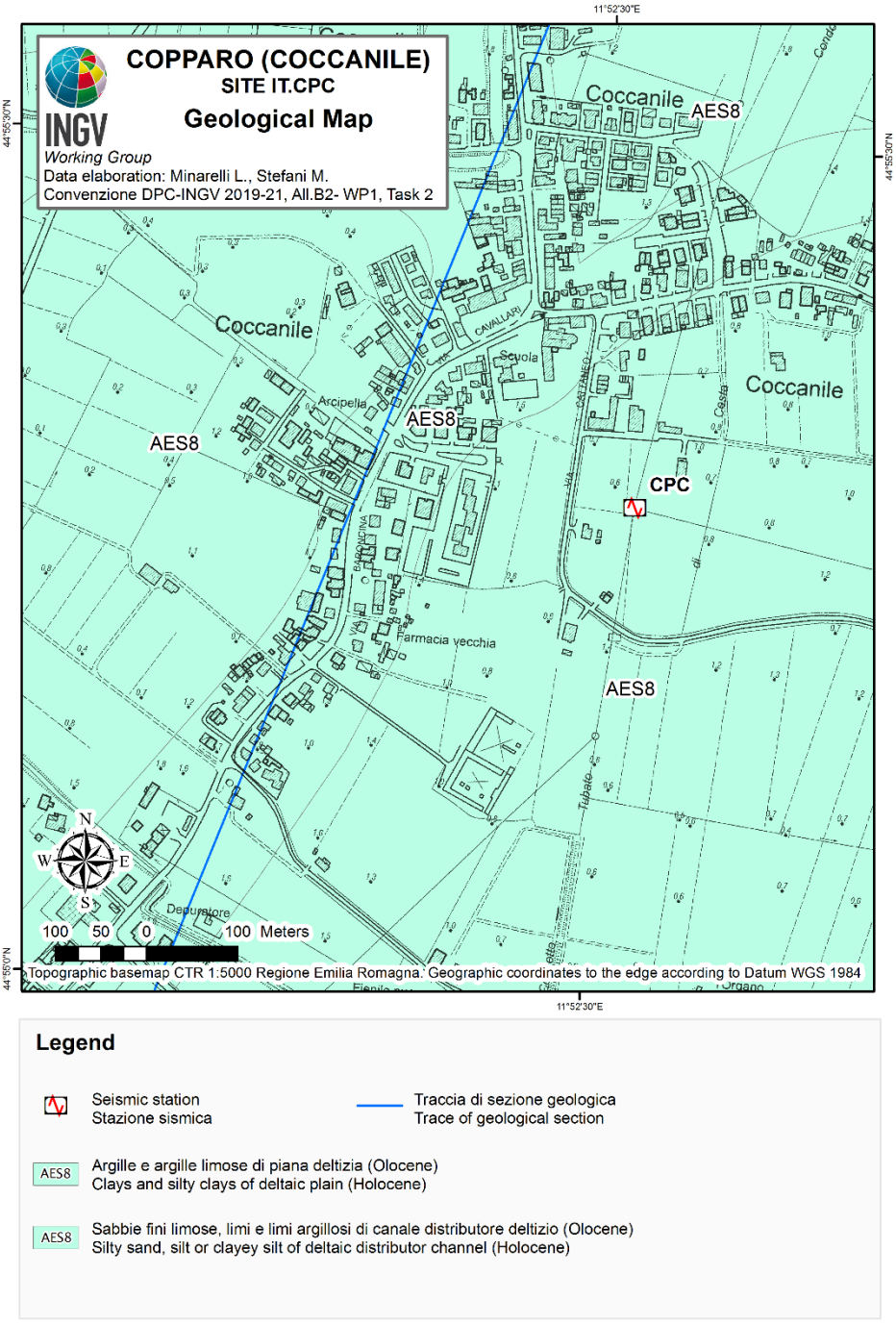

Figure 1. Geological map of the seismic station site IT.CPC. Scale 1:5.000. Geological units are mapped according to the nomenclature of the geological map of Italy 1:50.000. The 2D geological section (trace in blue line) is shown in Figure 6.

A3. LITHOTECHNICAL MAP

In Figure 2, the Lithotechnical Map is reported in a 1km x 1km square area around the station.

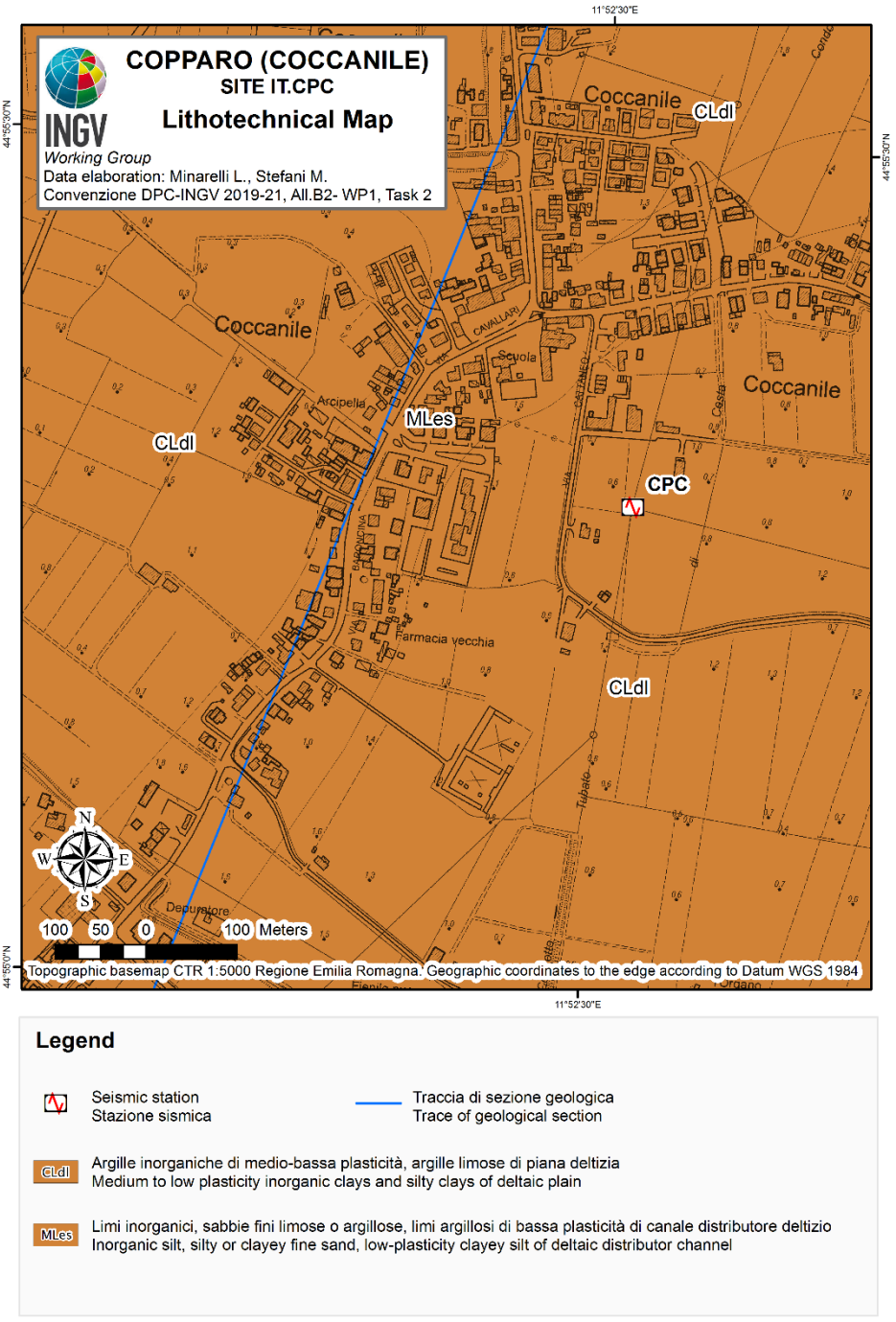

Figure 2. Lithotechnical map of the seismic station site IT.CPC. Scale 1:5.000. The lithotechnical units are attributed according to the nomenclature of the Seismic Microzonation study (Technical Commission SM, 2015). The 2D geological section (trace in blue line) is shown in Figure 6.

A4. SURVEY MAP

Figure 3 shows the Survey Map reporting both previous investigations and the geophysical surveys conducted by the INGV Working Group.

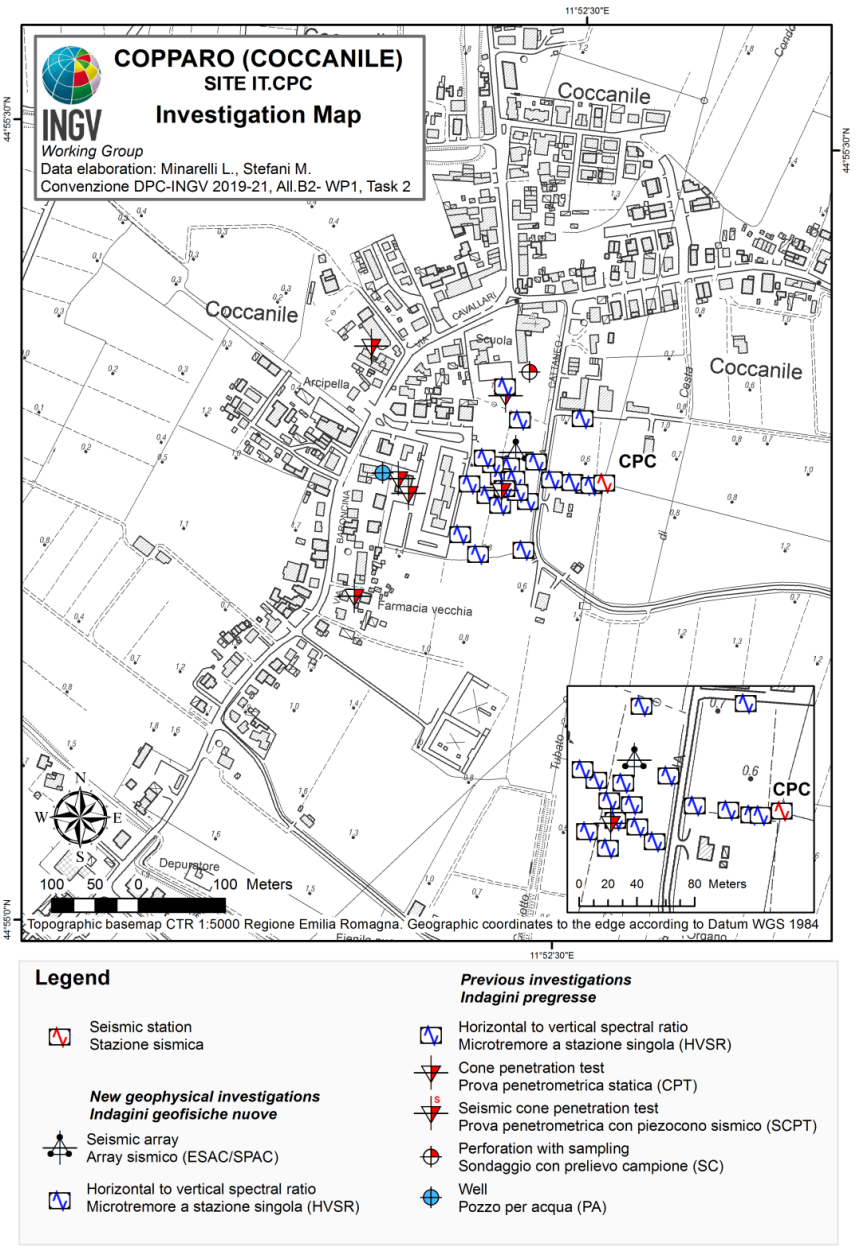

Figure 3. Map of the geophysical and geotechnical surveys made in the sector around the seismic station IT.CPC. Scale 1: 5.000. The box at the bottom right contains a zoom in representation of the station area. West of the station, the geophysical investigation conducted by INGV Working Group for the seismic characterization of the site have been performed (Convenzione DPC-INGV 2019-21, Allegato B2-WP1, Task B, Velocity profile at the seismic station report IT.CPC).

A5. GEOLOGICAL MODEL

5.1 General description

The seismic station is in the Coccanile village, at the north-west of Copparo, in the north-western portion of the Ferrara Province, at less than 1 meter above sea level. The site belongs to the delta plain of the River Po, developed over the foredeep basin of the Northern Apennines chain. The area is placed near the tectonic front of a complex structural fold and fault belt, forming the buried external portion of the Apennines chain, known as the Ferrara Arc (Pieri & Groppi, 1981). The fault system is part of the NE-verging external arc of the Northern Apennines chain. A tectonic pop-up, corresponding to the frontal thrust-fold belt of the buried chain, is developed a few kilometers to the south-west of the station site, which is located in a wide syncline area. The tectonic structures developed through late Neogene and Quaternary times and are covered by thick Quaternary sedimentary successions, which record a shallowing evolution, from open marine to continental environments. The Quaternary successions are affected by the differential subsidence induced by the tectonic deformation. The local deformation superposed to the regional subsidence gradient induced the highest subsidence values in the synclinal areas, whereas the lowest ones characterize the buried anticlines (Ghielmi et al. 2013; Vannoli et al. 2015, Stefani et al. 2018). The different subsidence rates determined great lateral variations in the stratigraphic thickness, depositional facies, and petrophysical properties (Figure 4).

The compressive stress-field affecting the tectonics structures is responsible for the seismic activity of the elongate, composite seismogenic source ITCS050 “Poggio Rusco-Migliarino” (DISS Working Group, 2018), present a few kilometers to the south of the station site. The fault system, developed at the north-eastern tip of the buried Northern Apennines chain, marks the most advanced, northeastern thrust with damaging seismogenic potential of the Apennines. No important historic earthquakes are known in the vicinity of the seismic station site, but the historic information recording potential of the area was poor, since, before the

19th century, the area was scarcely populated due to the presence of extensive marshes, today reclaimed.

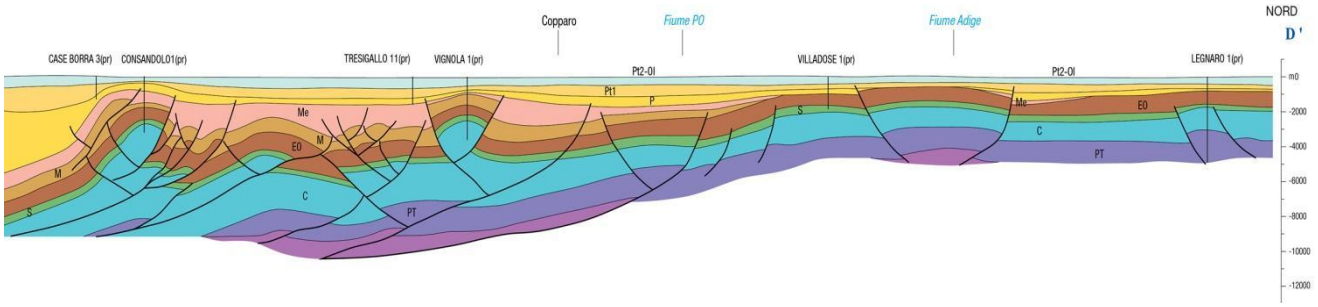

Figure 4. Structural profile (Martelli et al. 2017). The Permo-Miocene formations are detached from the metamorphic basement. Several complex anticline structures are involved in active compressive deformation and are associated with ramp overthrusts, interspaced by synclines.

The profile (Figure 4) is roughly elongated north-south and passes just a few kilometers to the east of the seismic station, which is located over the asymmetric syncline structure depicted in the profile, beneath the word "Copparo" . The complex overthrusting involving the Permo-Miocene sedimentary units detached from the metamorphic basement is clearly visible, as well as the great lateral variation in the stratigraphic thickness of the Plio-Quaternary successions. The large sediment thickness accumulated into the syncline area thins out between Copparo and Tresigallo, on the Vignola Well structural high, and, in the opposite direction, toward the Villadose and Adige highs.

The combined effect of the tectonic deformation pulses and of the Quaternary glacio-eustatic fluctuations generated a series of regional discordance surfaces, which are used as key levels to subdivide the sedimentary successions into allostratigraphy units, such as Synthems and Subsynthems (Emilia-Romagna Region and ENI/AGIP, 1998).

5.2 Geological Section

The seismic station is placed on a wide syncline developed at the front of the buried external portion of the Apennines Chain (see previous paragraph). No direct data on the station deep

subsurface are available, but a general structural and hydrostratigraphic framework can be inferred from the stratigraphic profile depicted in Figure 5, roughly stretching in a West-East direction (Molinari et al. 2007). The profile incorporates data from previously drilled wells and from bore geoelectric logs. The section was traced at about 10 km south to the seismic station, but the geological framework can be extrapolated to the discussed site, since the lateral stratigraphic gradient are low, and the gentle dip direction of beds is orthogonal to the perpendicular joining the seismometry site and the profile. The subsurface geology of the station site roughly corresponds to the one depicted in the profile between Sabbioncello and Tresigallo. From this segment the information used in the site underground interpretation were extracted, as discussed in paragraph 5.3. The thickening out the stratigraphic units eastward, moving out from the structural high of Casaglia-Pontelagoscuro, toward the Adriatic Sea, is clearly visible. The successions record a coastal progradation and shallowing evolution, from the aquifer complex B, mainly deposited into marine environments, to the mainly continental units of the aquifer complex A0, belonging to the AES8 Subsynthem. While interglacial highstand marine sand reach the Sabbioncelo area within the AES6 Subsynthem, they are confined to the eastern Comacchio area in the AES8 one.

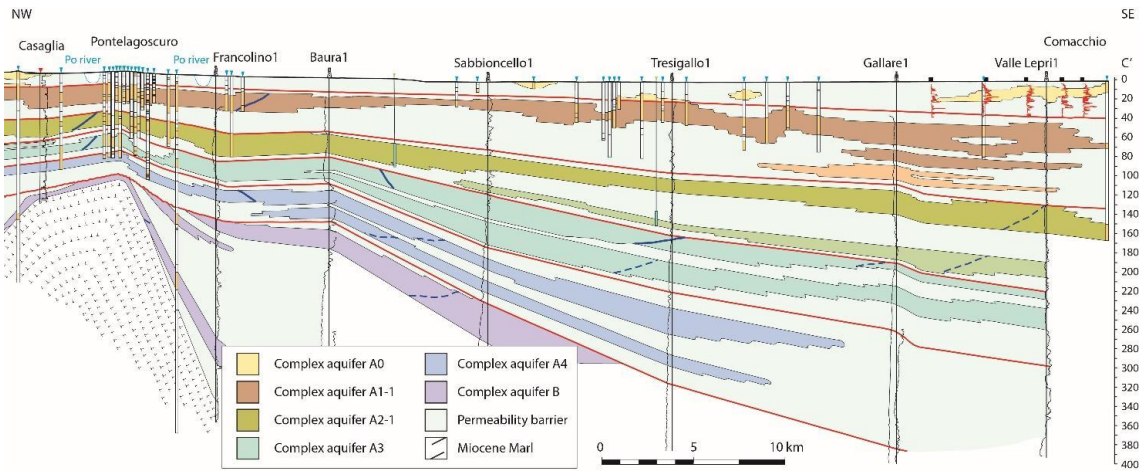

Figure 5. Schematic geological-hydrostratigraphic cross section, oriented in a NW-SE direction, showing the geometrical discordance relationships between the folded Neogene units and the Quaternary sedimentary infilling of the foredeep basin of the Northern Apennines chain (modified by Molinari et al. 2007). The seismic station site is located about 10 km at the north of the section.

5.3 Subsoil model

A subsurface geological model for the area surrounding the seismic station was developed, to the depth of about 320 m (Figure 6). The model is based on the integration of several sources of information, i.e., new geophysical investigations performed for the seismic characterization of the site, a new geological mapping of the outcropping geology, and the analysis of the available geotechnical investigation (Synthetis 2017). The whole of the published information was also collected, analyzed, and synthesized. The subsurface model is well constrained for the first 30 m of subsurface, thanks to the correlation of the cone penetration tests, available near the seismic station. The deeper part of the model is not as well constrained, since no direct coring is available in the area and therefore the information has been extrapolated from literature maps and geological profiles (Martelli 2021, Martelli et al. 2017, Molinari et al. 2007).

The first 21-22 m of subsurface belongs to the Subsintema di Ravenna (AES8), consisting of clay, silty clay, organic-rich clay and peats, mainly accumulated into an interdistributary area of the Po Delta. The shallow subsurface stratigraphy at the station consists only of fine-grained mud, with some minor granular intercalations in the lower portion of the Subsynthem, but not far to the west an elongated body of sand, infilling a minor delta channel of the Po is developed (Figure 6). The following interval (22 to approximately 90 m) belongs to the Villa Verucchio Subsynthem (AES7). The upper portion of the unit is better known than the lower one and consists of medium to coarse sand, deposited by the Po River input into a middle alluvial plain, mainly during synglacial times. The sand unit is about 20-25 m thick. The remaining portion of the Subsynthem is probably dominated by continental argillaceous mud, lacking major marine sand intercalations.

The underlying Bazzano Subsynthem (AES 6) follows (about 90-140 m). The upper interval is dominated by synglacial continental sands, the central one consists of mainly continental argillaceous mud. In the lower portion sand is again found, probably deposited into delta-estuarine environments. The depth of the AES6 unit base is placed according to the

hydrostratigraphic profile on Figure 5 (Molinari et al. 2007) and the seismotectonic map (Martelli et al. 2017).

The knowledge of the underlying units is ever more incomplete, but some good information derives from the regional framework. The interval between 140 and about 300 m consists of the lower portion of the Emiliano Romagnolo Superiore Synthem (AES), formed by intercalation of clay mud and sands, sedimented into coastal marine and alluvial plain environments and probably recording two glacial-interglacial eustatic cycles. The unit base is described at about 300 m also by the regional seismotectonic map (Martelli et al. 2017) and is matched with an angular unconformity near the anticline culmination, laterally grading into paraconformity contacts (Figure 5 modified by Molinari et al. 2007).

Between about 300 and 450 m, the Emiliano Romagnolo Inferiore Synthem (AEI) is here developed (Martelli 2021), probably here rich in marine deposits, again formed by sand and mud alternations. Because of the burial depth and compaction level of the unit, the lower Synthem probably already belongs to the seismic bedrock.

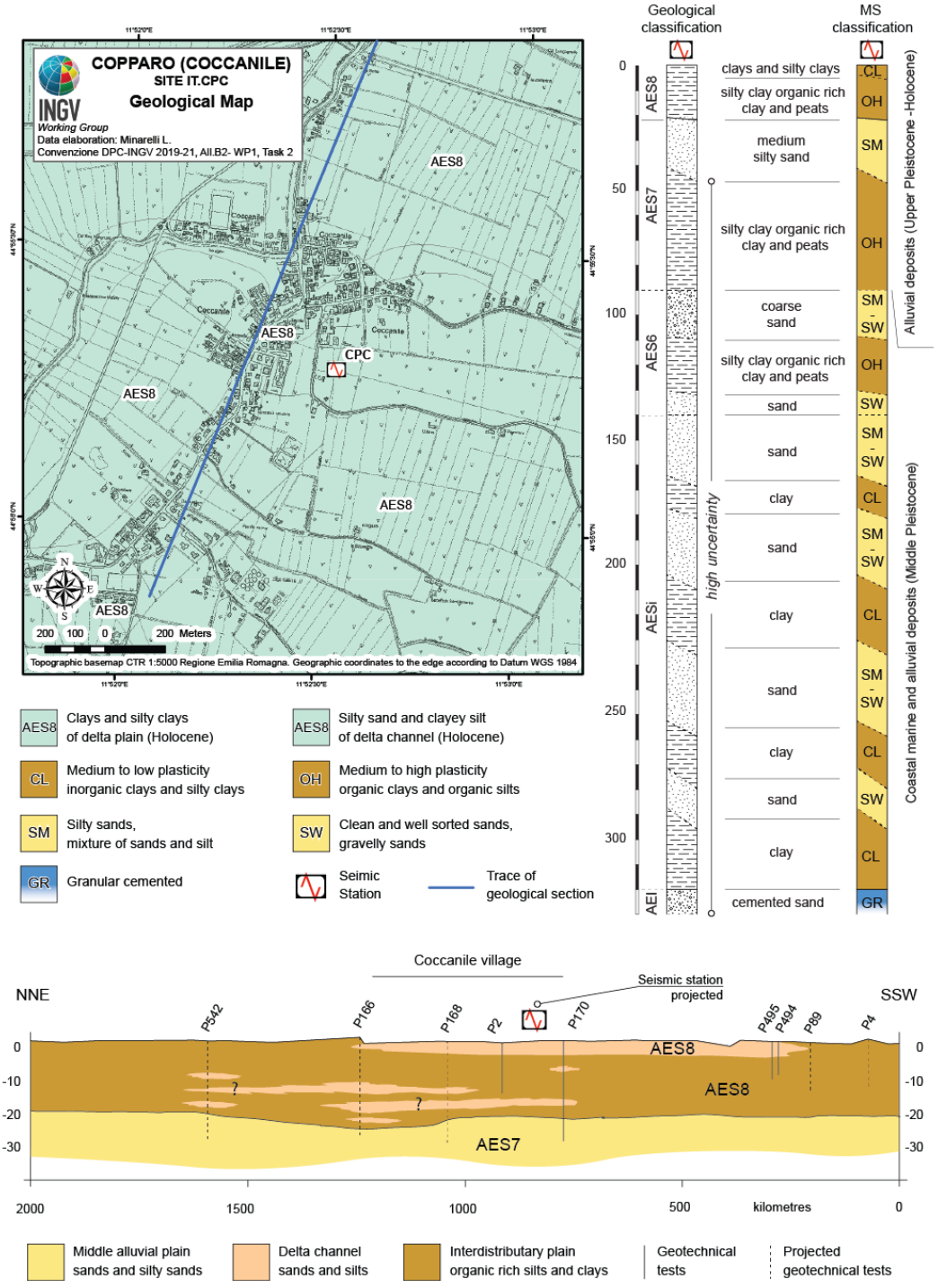

Figure 6. Bottom - Geological section crossing seismic station IT.CPC. Right - Subsoil model under the IT.CPC seismic station and classification according to the nomenclature of the geological map of Italy 1:50.000 and according to Seismic Microzonation (SM).

B. Vs profile

B1. GEOPHYSICAL INVESTIGATIONS

In this part of the report, we present the geophysical surveys and the results obtained for IT.CPC station.

Geophysical surveys are based on several ambient-vibration measurements next to the target station (Fig. 7). In detail we used i) a 2D array composed of 12 digitizers (Reftek130) coupled to three-components Lennartz velocimeters (Le3d5s with eigen-frequency of 0.2 Hz), which are arranged in a spiral-like geometry with a maximum aperture of about 200 m (AC stations in Fig. 7); ii) a 2D array composed of 24 vertical geophones (Geospace with eigen-frequency of 4.5 Hz) deployed along two main rings with a maximum aperture of 50 m (SC stations in Fig. 7); iii) additional 2D array composed of 9 stations equipped with triaxial geophones (4.5 Hz natural frequency, Terrabot stations by Sara Electronics; TC stations in Fig. 7).

Due to the site logistics, the major number of stations was deployed in the field on the left with respect to IT.CPC position, and a distance of about 70 m far from IT.CPC (see Fig.s 7 and 8). All the geophysical measurements were recorded on the 17th June of 2021 (very sunny day and no wind).

Duration of the ambient vibration measurements at AC and TC stations was larger than 3 hours and half. The SC geophones were coupled to a multi-channel system (Geode manufactured by Geometrics) recording about 2 hours and 45 minutes of ambient vibrations. The sampling rate was set to 250 sps for AC, TC and SC stations.

To assess the resonant frequency (f0) of the site, the horizontal-to-vertical (H/V) spectral analysis was calculated.
Using surface-wave analysis based on array techniques, we provide results also in terms of dispersion curves (DC). The observed curves were inverted to obtain the shear-wave velocity (Vs) profiles of the studied area. The obtained velocity models are suitable for determination of the average Vs velocity in the uppermost 30 m (Vs30) and assigning then the soil class category as prescribed by current Italian seismic code (NTC18) and Eurocode (EC08).

The software of analysis was *Geopsy* (http://www.geopsy.org; Wathelet et al. 2020).

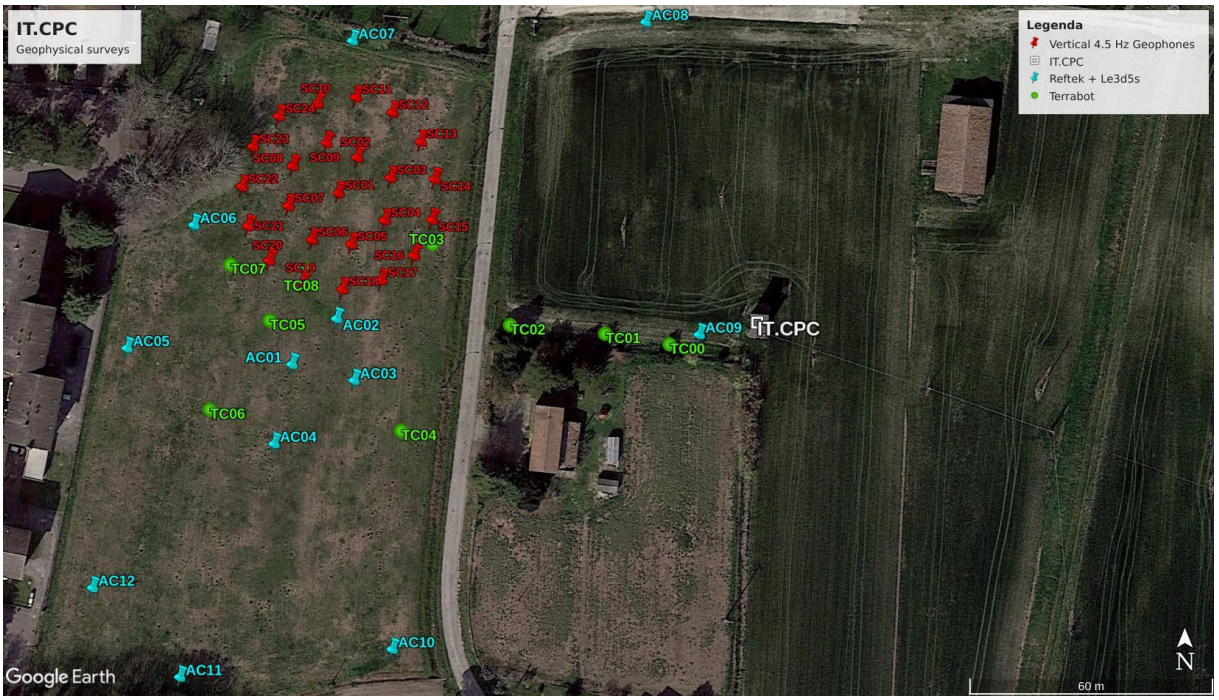

Figure 7. Plan view of the geophysical surveys in proximity of the IT.CPC station (white square). The coloured markers refer to different seismic equipment: Reftek 130 connected to Lennartz 3d 5s (from AC01 to AC12, cyano markers); Terrabot all-in-one stations (from TC00 to TC08, green circles); 4.5 vertical geophones (from SC01 to SC24, in red). Image by Google Earth http://www.earth.google.com.

Figure 8. Field picture where the majority of seismic stations were installed. The accelerometric station IT.CPC is installed in the Enel box (gray cabinet visible in the picture; the viewpoint of the photo is approximately from AC01 position towards IT.CPC).

1.1 H/V spectral ratio from seismic noise measurements

Figure 9 shows the actual H/V curves for the three-components seismic stations installed in the field (12 and 9 measurement points for AC and TC array, respectively). For all stations there is a good agreement of the H/V shapes, with H/V peaks with amplitude level between 2.5 and 3 in the frequency band 0.4-0.6 Hz. In this band, two near peaks with comparable amplitudes can be distinguished at 0.43 Hz and 0.56 Hz (Figs. 9a and 9b).

Interestingly the TC stations (Terrabot) have an eigen-frequency of 4.5 Hz, but in this case they are able to reproduce the same peaks around 0.4-0.6 Hz observed on AC stations that are equipped with Lennartz-5s sensors (i.e eigen-frequency of 0.2 Hz).

Additional peaks at lower frequency (i.e. < 0.2 Hz), if present, are not well resolved by our measurements. The sharp peak at 0.14 Hz of the TC stations is likely related to the instrumental response of the Terrabot. The peak at about 0.1 Hz observed on H/V curves of the AC stations is very scattered and with larger uncertainties. Fourier spectra of the three components of motion (EW, NS and Z) for all the stations are overlaid in Fig. 9c, confirming an amplified frequency band between 0.4-0.6 Hz where the horizontal components show a larger amplitude level than the vertical ones.

The rotated H/V spectral ratios are also very similar among the stations and do not show significant polarization effects (Fig. 9d; for simplicity we report the AC09 and TC00 stations which are located very close to IT.CPC) .

For the reasons above, we consider the f0 of IT.CPC equal to 0.43 Hz.

Please note that this f0 value is slightly different from the one present in Engineering Strong Motion archive (ESM https://esm-db.eu/; Luzi et al. 2020) at the moment of writing this report (0.36 Hz, see Fig. 10). The secondary peak at 4.36 Hz shown in the ESM (Fig. 10) is not present in our data, suggesting a possible anthropic cause of the 4.36 Hz peak during the older measurement.

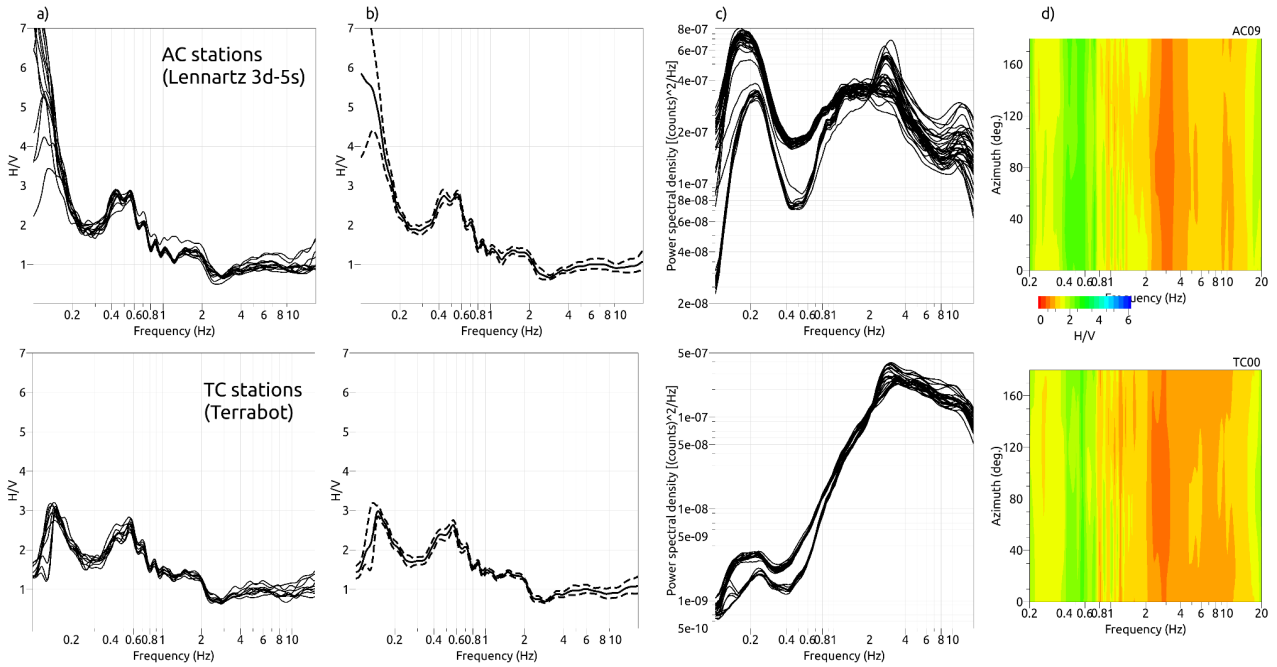

Figure 9. H/V spectral ratios (mean curves) are reported in (a) for all the stations (top and bottom panels refer to AC and TC stations, respectively). H/V curves averaged among all the stations are shown in (b) with uncertainties (the dashed curves are the mean plus/minus one standard deviation). Spectra of the horizontal (EW and NS) and Z components are overlaid in (c) . Directional H/V curves for AC09 and TC00 are shown in (d); the colour scale is proportional to the amplitude value of the H/V curves.

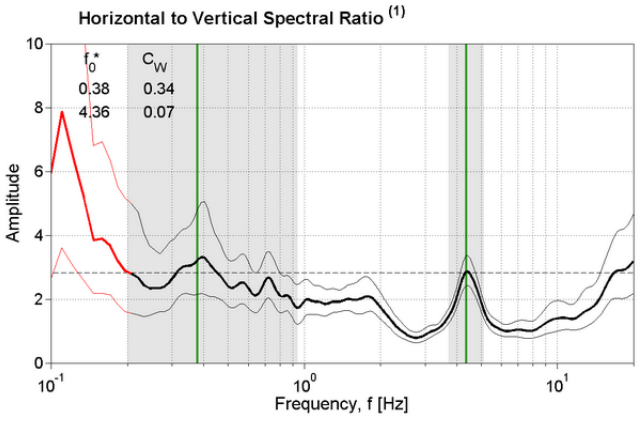

Figure 10. H/V spectral ratios reported on ESM archive (author of measurements DPC, record duration 60 min and instruments Lennartz3d-5s). The f0 is given in ESM at 0.38 Hz (https://esm-db.eu/), whereas the measurements shown in this report indicate a f0 equal to 0.43 Hz.

To extract the Rayleigh-wave ellipticity curve to be used in the surface-wave inversion, the Random Decrement Technique (Raydec; Hobiger et al. 2009) was applied to one station of AC array (AC09 was selected because the closest one to IT.CPC, see Fig. 7) for evaluating the relative contribution of surface and body waves in the H/V composition. Raydec method aims at enhancing the occurrence of Rayleigh waves and suppressing the contribution of body waves, taking into account the theoretical 90° phase shift between radial and vertical components of the Rayleigh wave. The Raydec ellipticity curve of AC09 (Fig. 11) has a shape similar to the H/V curves already shown in Fig. 9a for the AC array. The ellipticity curve still shows the two peaks at 0.43 and 0.56 Hz (ashed curve in Fig. 11), with a lower level of amplitude with respect to the corresponding H/V curve. The amplitude difference between the ellipticity and H/V curves is almost constant (a factor of about 1.4) in the frequency range 0.2-1 Hz.

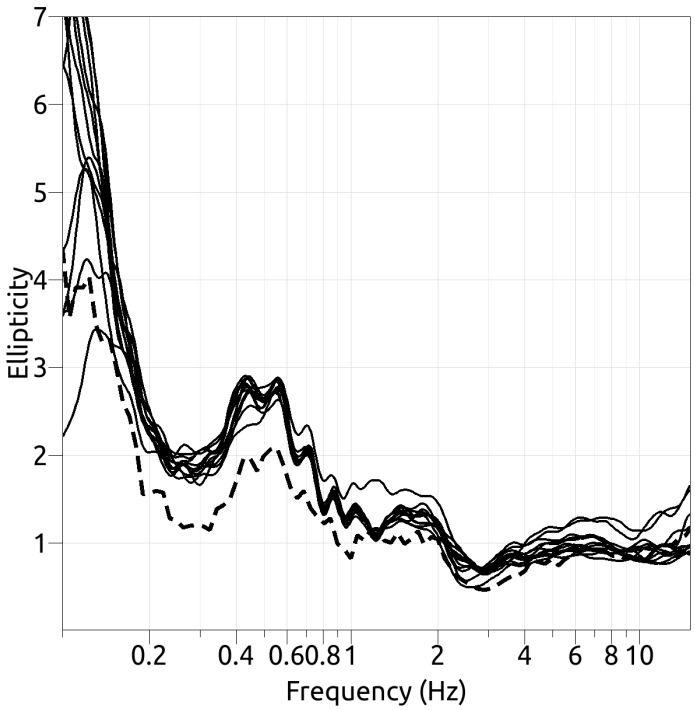

Figure 11. Comparison between the mean H/V spectral ratios of AC array (continuous black curves; the same curves in Fig. 9a) and the ellipticity curve after the Raydec analysis of AC09 station (dashed curve).

1.2 2D Array analysis

The ambient vibration data were processed using the *GEOPSY* software tools (www.geopsy.org) in order to extract the surface-wave dispersion by applying to the seismic signals frequency-wavenumber (FK) or spatial autocorrelation analysis (SPAC).

1.2.1 Vertical geophones (SC array)

SC stations (Fig. 7) are composed of 24 vertical geophones deployed along two main rings (with maximum radius of 25 m). Passive data (or noise) were recorded and synchronized using one multichannels system (Geode manufactured by Geometrics) that acquired continuous time windows of 240 s length (4 minutes) at a sampling rate of 4 ms (250 Hz), for a total duration of noise recordings of about 2 hours and 45 minutes.

The data of the SC array were analysed in terms of conventional frequency-wavenumber (FK) analysis applied to the vertical component. Figure 12 shows the dispersion results; the apparent phase-velocities are varying from about 280 (at 2.5 Hz) to 200 m/s (at 3.5 Hz), and with an asymptotic velocity value of about 130 m/s starting from 7 Hz up to 25 Hz. A possible higher mode of Rayleigh waves can be recognized in Fig. 12 in the frequency band 6-10 Hz with apparent phase-velocity ranging from 250 to 210 m/s.

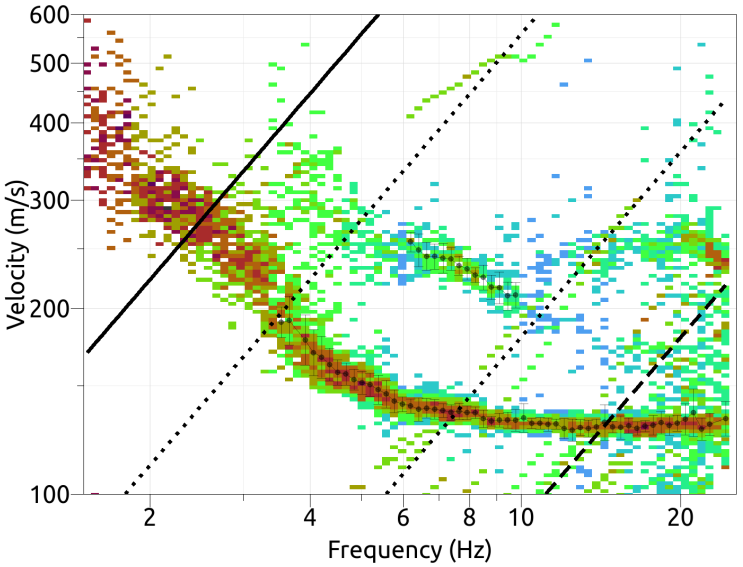

Figure 12. FK analysis performed on passive data acquired by the SC array of vertical geophones. Results are shown in the velocity-frequency plan; the theoretical resolution (Kmin/2, Kmin) and alias limits (Kmax/2, Kmax) are overlaid as black lines.

A Cross-Correlation (CC) method was also applied to the SC array using an ad hoc software (Vassallo et. al. 2019). Fig. 13 shows the computed cross-correlations functions (organized according to the distance between station pairs) and the results of the velocity analysis performed on CCs. Specifically, the SC data were processed using one-bit normalization and spectral whitening (Bensen et al. 2007). Then, the cross-correlation functions were computed for the processed traces at the different station pairs of arrays (Fig. 13 top panel). To compute the dispersion curve of the seismic signals, we applied a Constant Velocity Stack (CVS) analysis (Yilmaz, 1987) to the CCs functions (Fig. 13 bottom panel). The cross-correlation functions were filtered in different frequency bands starting from 3 to 40 Hz. Then the cross-correlation functions were shifted back in time according to different constant velocities starting from 50 m/s until 600 m/s using a velocity step of 10 m/s. For each frequency band and velocity correction, a Phase-Weighted Stack was computed, and the maximum of the stack function provided the velocity of surface waves at the considered frequency. The dispersion curve (black line in Fig. 13bottom) is identified on the basis of the maximum value of the stack function at each frequency, and shows a good agreement with the results of the f-k analysis.

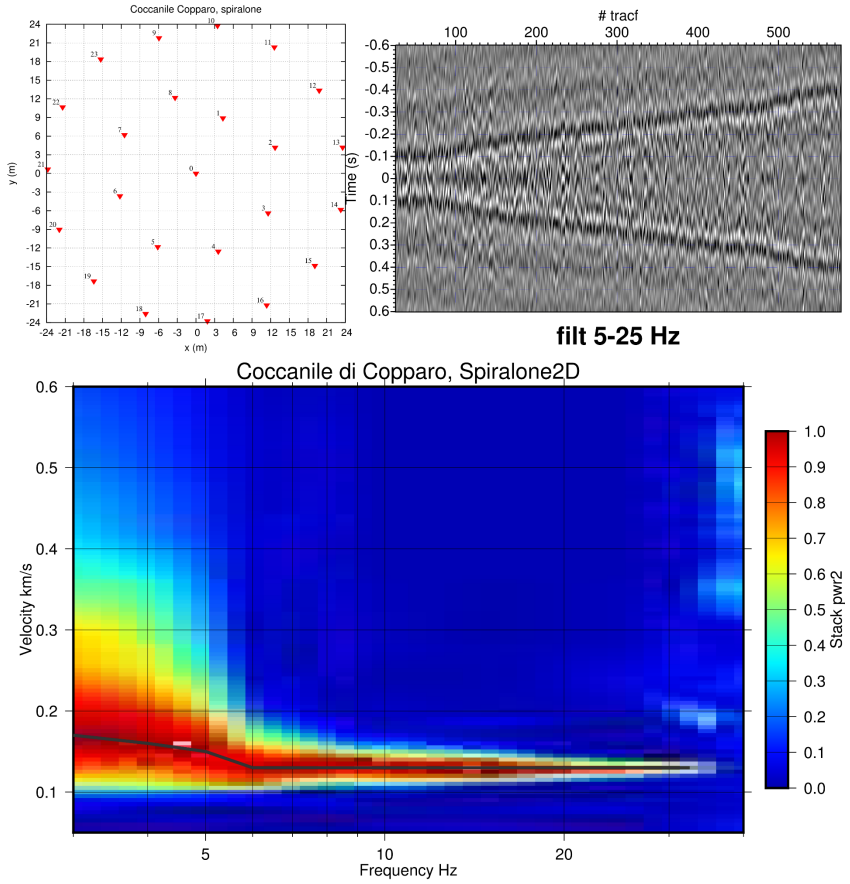

Figure 13. Cross-Correlation (CC) analysis performed on data acquired by the SC array of vertical geophones. The top panel shows the geometry of the array, and the CC functions filtered in the frequency band 5-25 Hz. The traces in CC section are organized for increasing interdistance (#tracf). The bottom panel shows the results of Constant Velocity Stack (CVS) analysis;the black curve follows the maxima of the stack function over frequency.

1.2.2 Lennartz-5s (AC array) and Terrabot stations (TC array)

We applied the high-resolution Radial-Transverse BeamForming (RTBF) analysis to three-components data of the AC and TC arrays (see Fig. 7), in order to derive Rayleigh and Love dispersion curves (Fig. 13) searching from the FK maxima in the wavenumber plane (kx, ky) as implemented the *Geopsy* tool (Wathelet et al. 2018). The frequency range of analysis for each selected array was based on the resolution and alias theoretical limits. The Rayleigh and Love

phase dispersion curves of the AC and TB arrays (Fig. 14) are in good agreement in a frequency range from about 1 to 10 Hz. Rayleigh-wave DCs show velocity of 340 m/s for the theoretical lower frequency limit at 1.2 Hz (where the estimated dispersion curve matches the resolution curve of the AC array; Fig. 14a top). At higher frequencies, the velocity values are in agreement with the one estimated by the SC array. A higher mode of Rayleigh waves is evidenced especially in the AC array (Fig. 14a top) in the frequency band 1.4-4 Hz. The Love DC shows lower velocities than Rayleigh DC up to 4 Hz (Fig.s 14b and 14c); for larger frequencies the Rayleigh and Love waves share approximately the same values of phase-velocity (Fig. 14c). We also repeated an RTBF analysis by merging data from the AC and TC arrays that run concurrently for a couple of hours. Although less clear than the single processing of the AC and TC arrays, the results of the merged array (AC+TC; not shown here) confirm the dispersion curves estimated in Fig. 14.

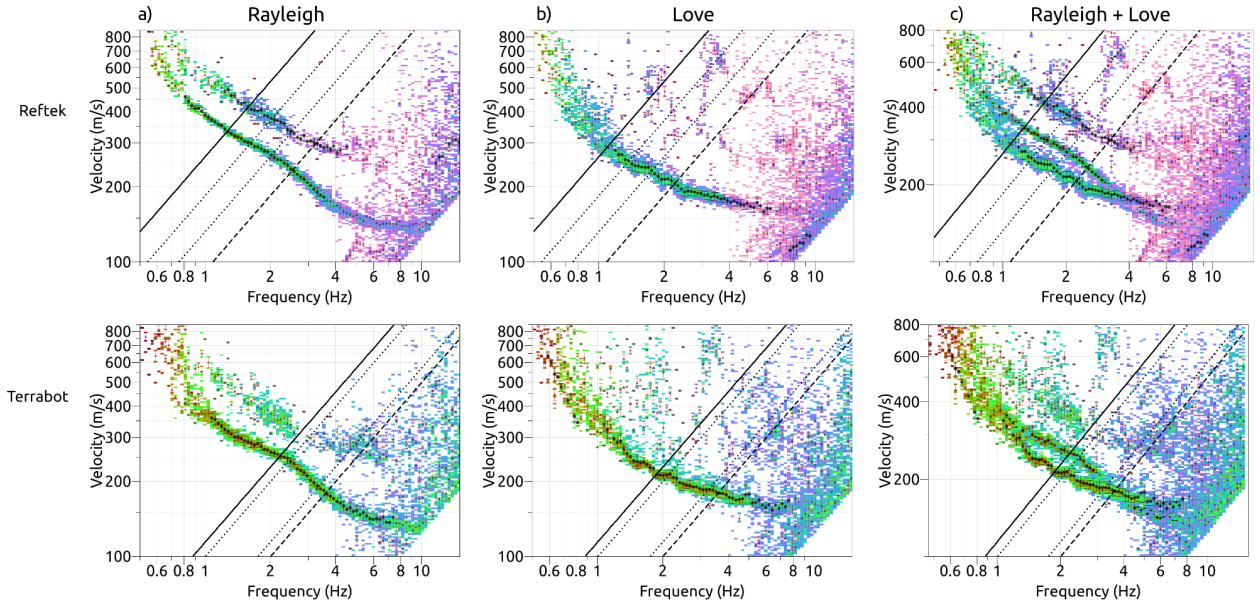

Figure 14. RTBF analysis performed on 3C data for the 2D array of Lennartz-5s (AC, top panel) and Terrabot (TC, bottom panel). The resulting dispersion curves for Rayleigh and Love waves are shown in a) and b), respectively. Rayleigh and Love-waves dispersion curves are overlaid in c).

A cross-correlation analysis was also performed on vertical signals of the AC array (composed of Lennarts-5s). The Rayleigh DC curve from SPAC analysis is found in between the fundamental and first higher Rayleigh mode observed on the FK results (Fig. 15). Therefore the DC from SPAC analysis was not considered during the inversion step.

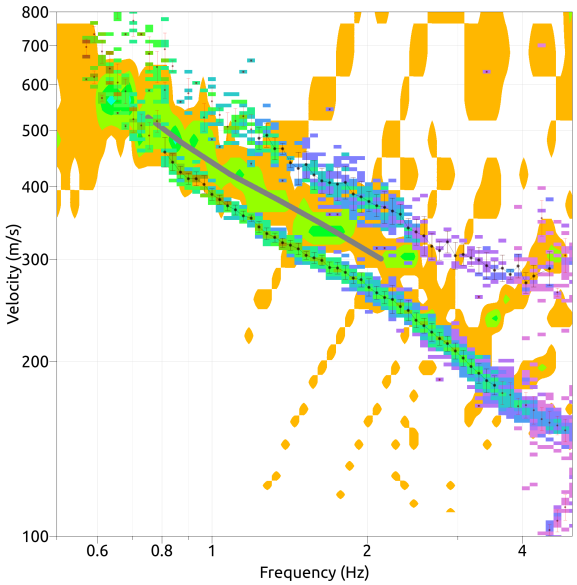

Figure 15. SPAC analysis performed on vertical components for the AC array. The estimated dispersion curve from SPAC analysis (thick grey curve) was found in between the fundamental and first higher-mode of Rayleigh waves resulting from the F-K RTBF analysis (picked black circles). For this reason the SPAC dispersion was not considered in the next.

B2. SEISMIC VELOCITY MODEL

1D seismic velocity model

To proceed in the inversion step, we extract a combined dispersion curve integrating the results from the array analysis shown in Fig.s 12, 13 and 14.
The final dispersion and ellipticity curve used as target in the inversion procedure are shown in Fig. 16. In detail for the DCs, we consider the fundamental and first higher mode of Rayleigh waves (R0 and R1 in Fig. 16a, respectively) together with the fundamental mode of Love waves (L0 in Fig. 16a). The FK analyses discussed above provide the dispersion curves in the frequency band within 1-10 Hz, whereas the CC analysis gives the velocity values above 10 Hz for the R0 curve (Fig. 16a). For the Rayleigh-wave ellipticity curve (Fig. 16b), we consider the Raydec analysis as shown in Fig. 11 in the frequency band 0.3-1 Hz.

The models derived from the inversion step (by *dinver* tool of *Geopsy* code) are shown in Fig. 17. We tested several model parameterizations composed of main soft layers over halfspace, including parameterizations that allow a Vs increasing with depth following a linear-law or a power-law. Based on the available information on the geological structure of the area (see the geological section of this report), we found reliable velocity models considering a parameterization of 4 uniform layers over halfspace (Fig. 17). The velocity contrasts are found at depths of about 10, 30, 140 and 300 meters (Fig.s 17e, 17f and 17g), where the Vs values increase respectively from 140 to 200 m/s, from 200 to 330 m/s, from 330 to 550 m/s, and from 550 m/s to 800 m/s. The two major impedance contrasts, corresponding to significant increases in the shear wave velocities, correlate to the bases of the Bazzano Subsystem (AES6) and of the Emiliano-Romagnolo Superiore Synthema (AESi). The stratigraphic bases depths were extrapolated from literature data (Martelli 2021, Martelli et al. 2017, Molinari et al. 2007), and are in good agreement with those of the major velocity contrasts identified through geophysical measurements.

From microzonation activity of the area, a shallow velocity profile up to a depth of 30 m was already available; it was from a Seismic Cone Penetration Test (SCPT) reported as black curve in Fig.s 17f and 17g. The models from surface-wave inversion for the uppermost 30 m match rather well the average Vs values, although are not able to follow the thin multiple variations of velocity with depth indicated by the SCPT (Fig. 17g).

The best-fit velocity models, extracted from the ensemble of the possible solutions produced by the joint inversion, are shown in Figure 18 and Table 5.

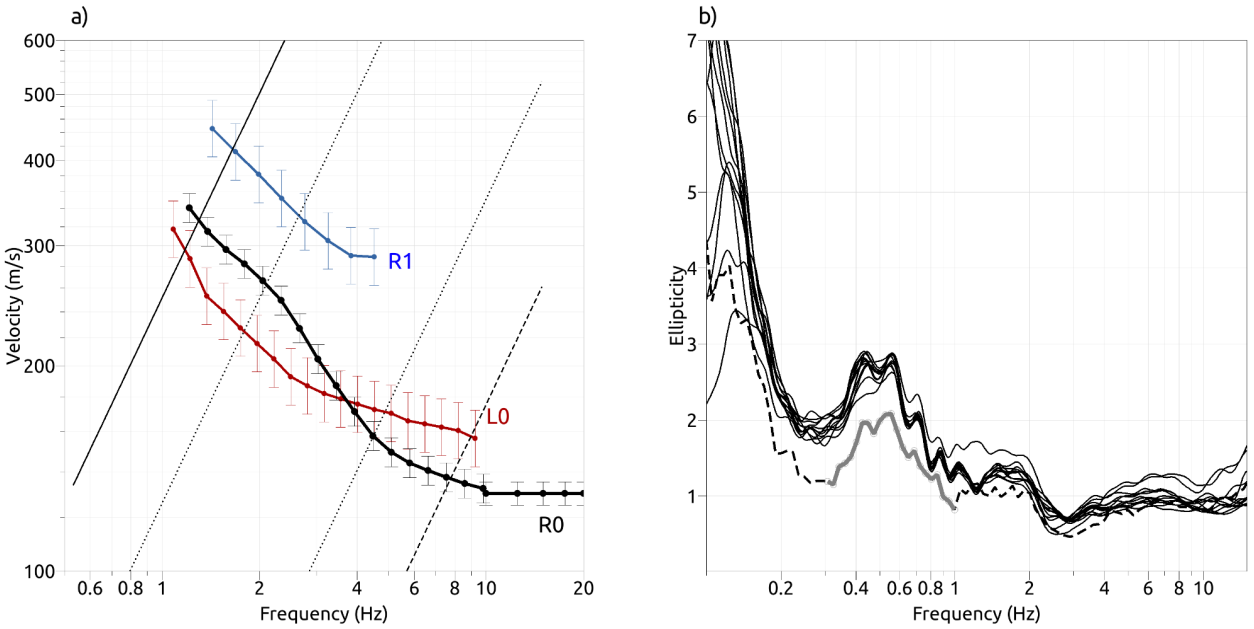

Figure 16. The final dispersion curves selected for the inversion step are shown on the a panel. R0 and R1 indicate the fundamental and first-higher mode of Rayleigh waves; L0 indicates the fundamental mode of Love waves. The theoretical resolution (Kmin/2, Kmin) and alias limits (Kmax/2, Kmax) of AC plus TC array are overlaid as black lines. The target Rayleigh-wave ellipticity assumed in the joint inversion is the grey continuous curve on the b panel (resulting from the Raydec analysis in the frequency band 0.3-1 Hz). The mean H/V spectral ratios of the AC array (continuous black curves; see Fig. 11) are reported in the plot for comparison with the ellipticity (grey curve).

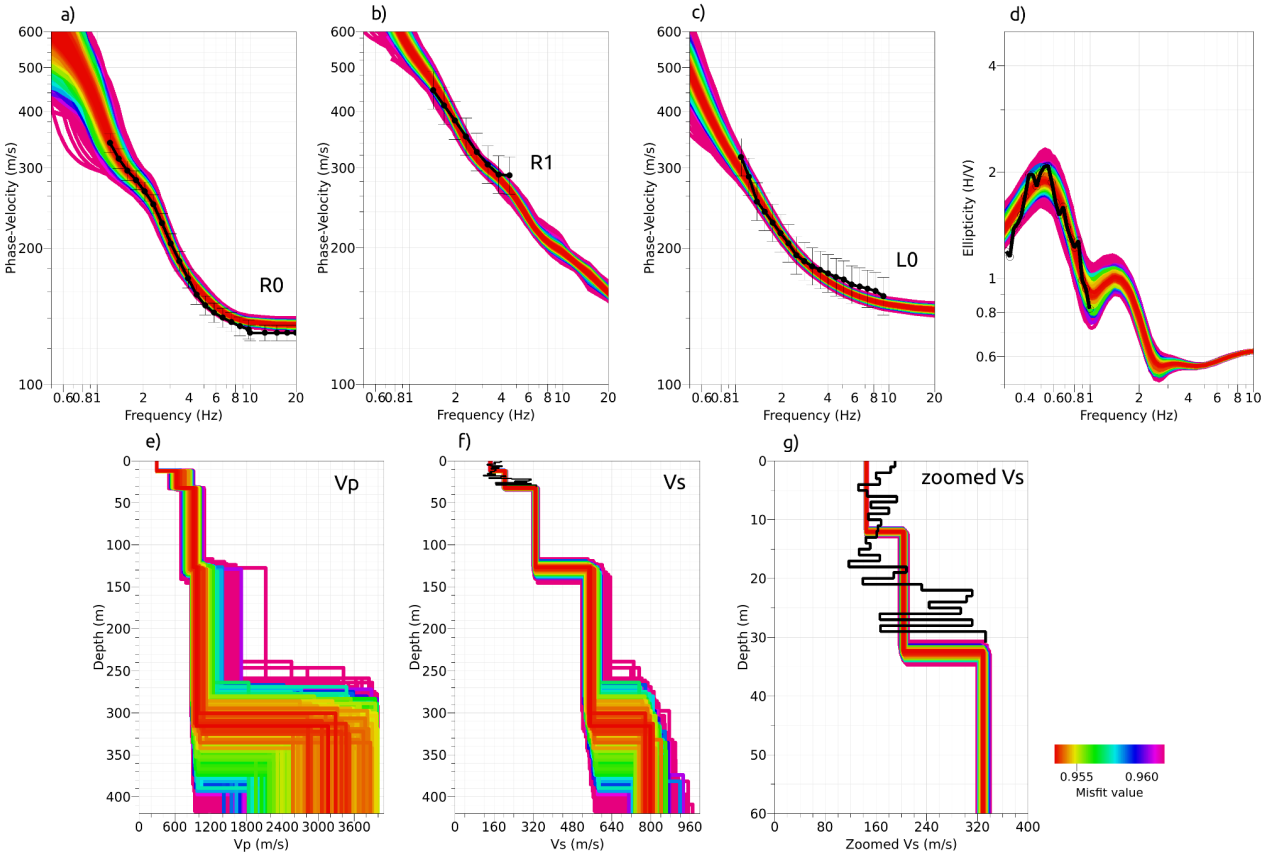

Figure 17. Models after the joint inversion of the dispersion and ellipticity curves (field curves are in black colour; the rainbow scale is proportional to the misfit between field and theoretical curves). The dispersion curves of R0 (fundamental Rayleigh mode), R1 (first higher Rayleigh mode) and L0 (fundamental Love mode) are shown in panels a, b and c respectively. The R0 ellipticity models are shown in panel d. The compressional (Vp) and shear-wave velocity (Vs) profiles are shown in panels e and f, respectively. A zoomed Vs profile is shown in g, with the black profile given by a SCPT velocity profile available from microzonation studies. The best velocity models are presented in Fig. 18.

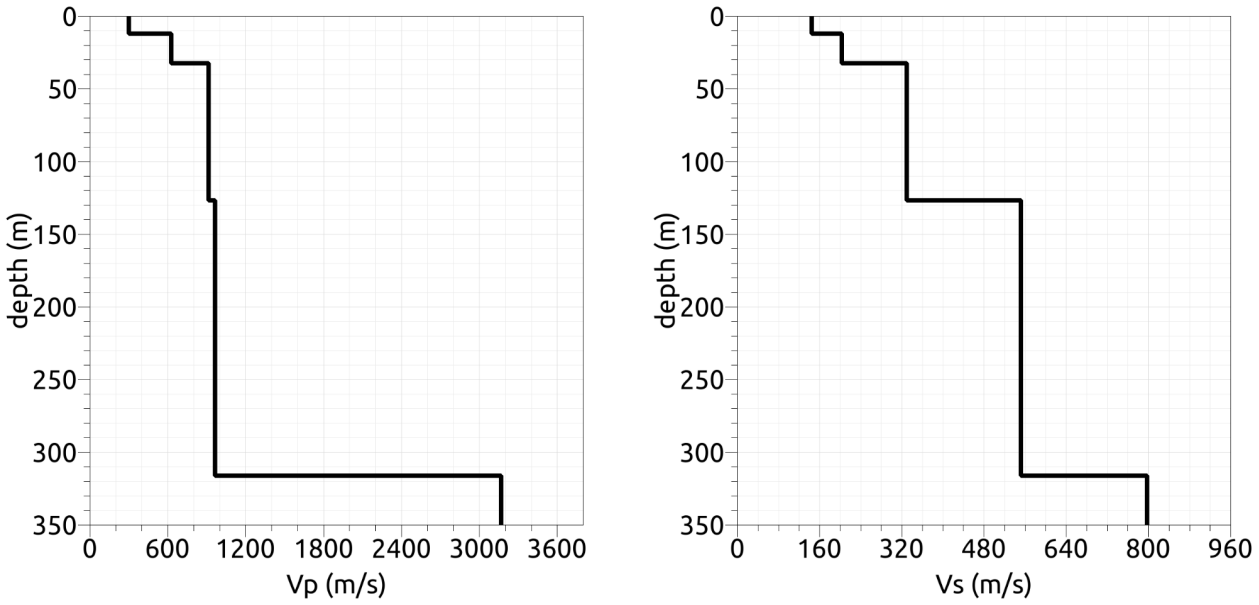

Figure 18. Best Vp and Vs models (extracted from Fig.s 17e and 17f).

Table 5. Best-fit model

From (m)	To (m)	Thickness (m)	Vs (m/s)	Vp(m/s)
0	12.3	12.3	145	300
12.3	32.6	20.3	203	627
32.6	126.7	94.1	329	913
126.7	317	190	552	964
317	1317	1000	797	3166

B3. CONCLUSIONS

Surface-wave analysis at IT.CPC station indicates a site of soil class D (Table 6). The best Vp and Vs models (i.e. lowest misfit) resulting from the inversion are proposed in Fig. 18 and Table 5.

HV noise spectral ratios show peaks in the frequency band 0.4-0.6 Hz, although we cannot exclude additional lower resonance frequencies not resolved from the resolution of our measurements.

2D passive arrays provide clear dispersion curves in the frequency range 1-30 Hz; the joint inversion of DCs and ellipticity curve gives the Vs models of Fig.s 17 and 18 with a bottom layer found at a depth of 317 m (Table 5).

The V_{S30} retrieved from the best inverted model is 175 m/s (Table 6), therefore IT.CPC is classified following EC8 as soil class D also taking into account the geological information (see paragraph 5.3). Following the definition of $V_{S,eq}$ within NTC18 and because the bedrock (Vs > 800 m/s) is reached at a depth above 30 m, the $V_{S,eq}$ is equivalent to V_{S30} and the soil class remains D (Table 6).

The station site of Coccanile (CPC) is characterized by low Vs values and by an engineering bedrock reached at great depth (317 m in our best-fit models), as occurs in a large part of the Po Valley, where the subsoil is composed of thick, non-lithified Quaternary sedimentary successions.

Table 6. Soil Class following EC8 and NTC18 .

V_{S30} (EC8)	**Soil Class**
175 m/s	D

$V_{S,eq}$ (NTC18)	**Soil Class**
175 m/s	D

REFERENCES

Bensen, G.D., Ritzwoller, M.H., Barmin, M.P., Levshin, A.L., Lin, F., Moschetti, M.P., Shapiro, N.M. and Yang, Y., (2007). Processing seismic ambient noise data to obtain reliable broad-band surface wave dispersion measurements" Geophysical journal international, 169(3), pp.1239-1260.

Carta Geologica d'Italia in scala 1:100.000 (1955). Foglio 76 - Ferrara. ISPRA http://sgi.isprambiente.it/geologia100k/mostra_foglio.aspx?numero_foglio=76

Carta Geologica d'Italia alla scala 1:50.000 (2009) - Foglio 187 – Codigoro. ISPRA – Servizio Geologico d'Italia - Regione Emilia-Romagna.
https://www.isprambiente.gov.it/Media/carg/187_CODIGORO/Foglio.html

D'Amico, M., Felicetta, C., Russo, E., Sgobba, S., Lanzano, G., Pacor, F., Luzi, L. (2020). Italian Accelerometric Archive v 3.1 - Istituto Nazionale di Geofisica e Vulcanologia, Dipartimento della Protezione Civile Nazionale. doi: 10.13127/itaca.3.1

DISS Working Group (2018). Database of Individual Seismogenic Sources (DISS), Version 3.2.1: A compilation of potential sources for earthquakes larger than M 5.5 in Italy and surrounding areas. http://diss.rm.ingv.it/diss/, *Istituto Nazionale di Geofisica e Vulcanologia; DOI:10.6092/INGV.IT-DISS3.2.1.*

EC8: European Committee for Standardization (2004). Eurocode 8: design of structures for earthquake resistance. P1: General rules, seismic actions and rules for buildings. Draft 6, Doc CEN/TC250/SC8/N335.

Ghielmi, M., Minervini, M., Nini, C., Rogledi, S. and Rossi. M. (2013). Late Miocene–Middle Pleistocene sequences in the Po Plain - Northern Adriatic Sea (Italy): The stratigraphic record of modification phases affecting a complex foreland basin, Marine and Petroleum Geology, Special Issue: The Geology of the Periadriatic Basin and of the Adriatic Sea, 42, 50-81; doi:10.1016/j.marpetgeo.2012.11.007.

Hobiger, M., Bard, P.Y., Cornou, C. and Le Bihan, N. (2009). Single station determination of Rayleigh wave ellipticity by using the random decrement technique (RayDec), Geophysical Research Letters, 36(14).

Luzi, L., Lanzano, G., Felicetta, C., D'Amico, M. C., Russo, E., Sgobba, S., Pacor, F., & ORFEUS Working Group 5 (2020). Engineering Strong Motion Database (ESM) (Version 2.0). Istituto Nazionale di Geofisica e Vulcanologia (INGV). https://doi.org/10.13127/ESM.2

Martelli, L. (2021). Assessment of Seismic Bedrock in Deep Alluvial Plains. Case Studies from the Emilia-Romagna Plain. Geosciences 2021, 11, 297. https://doi.org/10.3390/geosciences11070297

Martelli, L., Bonini, M., Calabrese, L., Corti, G., Ercolessi, G., Molinari, F. C., Piccardi, L., Pondrelli, S., Sani, L., and Severi, P. (2017). Carta sismotettonica della Regione Emilia-Romagna e aree limitrofe, scala 1:250.000 (edizione 2016). Con note illustrative, Regione Emilia-Romagna, SGSS; CNR, IGG sez. FI; Università degli Studi di Firenze, DST; INGV sez. BO. D.R.E.AM. Italia.

Molinari, F. C., Boldrini, G., Severi, P., Dugoni, G., Rapti Caputo, D. & Martinelli G., (2007). Risorse idriche sotterranee della Provincia di Ferrara. In: Dugoni G. & Pignone R. (Eds.), Risorse idriche sotterranee della Provincia di Ferrara. DB-MAP, Firenze, 7-61.

Norme Tecniche per le Costruzioni (NTC08). Ministero delle infrastrutture e dei Trasporti (2008). Decreto Ministero Infrastrutture. GU Serie Generale n. 29 del 04-02-2008 - Suppl. Ordinario n. 30.

Norme Tecniche per le Costruzioni (NTC18). Ministero delle infrastrutture e dei Trasporti (2018). Decreto Ministero Infrastrutture. GU Serie Generale n. 42 del 20-02-2018 – Suppl. Ordinario n. 8.

Pieri, M., Groppi, G. (1981). Subsurface geological structure of the Po Plain, Italy. Consiglio Nazionale delle Ricerche, Progetto finalizzato Geodinamica, sottoprogetto Modello Strutturale, pubbl. No. 414, Roma, 13p.

Regione Emilia- Romagna – Geoportale – https://geoportale.regione.emilia-romagna.it/

Regione Emilia-Romagna e ENI-AGIP, (1998). Riserve idriche sotterranee della Regione Emilia-Romagna. A cura di G. M. Di Dio. Regione Emilia-Romagna, ufficio geologico – ENI-Agip, Divisione Esplorazione e Produzione. S.EL.CA., Firenze, pp 120.

Stefani, S., Minarelli, L., Fontana, A., Hajdas, I., (2018). Regional deformation of late Quaternary fluvial sediments in the Apennines foreland basin (Emilia, Italy). Int. J.Earth Sci. 107 (7), 2433–2447. https://doi.org/10.1007/s00531-018-1606-x.

Synthesis (2017). Studio di Microzonazione Sismica di terzo livello del Comune di Copparo (FE). https://geo.regione.emilia-romagna.it/schede/pnsrs/index.jsp?id=38007

Technical Commission SM (2015). Commissione Tecnica per la Microzonazione Sismica 2015. Microzonazione sismica. Standard di rappresentazione e archiviazione informatica, Versione 4.0b (Commissione tecnica inter-istituzionale per la MS nominata con DPCM 21 aprile 2011).

Vannoli, P., Burrato, P., Valensise, G. (2015). The seismotectonics of the Po Plain (Northern Italy): tectonic diversity in a blind faulting domain. Pure Appl Geophys 172:1105–1142. doi:10.1007/s00024-014-0873-0

Vassallo, M., De Matteis, R., Bobbio, A., Di Giulio, G., Adinolfi, G.M., Cantore, L., Cogliano, R., Fodarella, A., Maresca, R., Pucillo, S. and Riccio, G. (2019). Seismic noise cross-correlation in the urban area of Benevento city (Southern Italy)" Geophysical Journal international, 217(3), pp.1524-1542.

Wathelet, M., Guillier, B., Roux, P., Cornou, C. and Ohrnberger, M., (2018). Rayleigh wave three-component beamforming: signed ellipticity assessment from high-resolution frequency-wavenumber processing of ambient vibration arrays, Geophysical Journal international, 215(1), pp.507-523.

Wathelet, M., Chatelain, J.L., Cornou, C., Giulio, G.D., Guillier, B., Ohrnberger, M. and Savvaidis, A., (2020). Geopsy: A user-friendly open-source tool set for ambient vibration processing. Seismological Research Letters, 91(3), pp.1878-1889.

Yilmaz O. (1987). Seismic data processing in Investigations in Geophysics, 2: Soc. Expl. Geophys, series Eds., eds Doherty S.M., Neitzel E.B.

INGV contributes, within the limits of its skills, to the evaluation of seismic and volcanic hazard in the Country, according to the mode agreed in the ten-year program between INGV and DPC February 2, 2012 (Prot. INGV 2052 of 27/2/2012), and to the activities planned as part of the National Civil Protection System. In particular, this document1 has informative purposes concerning the observations and the data collected from the monitoring and observational networks managed by INGV. INGV provides scientific information using the best scientific knowledge available at the time of the drafting of the documents produced; however, due to the complexity of natural phenomena in question, nothing can be blamed to INGV about the possible incompleteness and uncertainty of the reported data.
INGV is not responsible for any use, even partial, of the contents of this document by third parties and any damage caused to third parties resulting from its use. The data contained in this document is the property of the INGV.
This study has benefited from funding provided by the Italian Presidenza del Consiglio dei Ministri - Dipartimento della Protezione Civile (DPC). This paper does not necessarily represent DPC official opinion and policies.

Esclusione di responsabilità e limiti di uso delle informazioni
L'INGV, in ottemperanza a quanto disposto dall'Art. 2 del D.L. 381/1999, svolge funzioni di sorveglianza sismica e vulcanica del territorio nazionale, provvedendo all'organizzazione della rete sismica nazionale integrata e al coordinamento delle reti sismiche regionali e locali in regime di convenzione con il Dipartimento della Protezione Civile.
L'INGV concorre, nei limiti delle proprie competenze inerenti la valutazione della Pericolosità sismica e vulcanica nel territorio nazionale e secondo le modalità concordate dall'Accordo di programma decennale stipulato tra lo stesso INGV e il DPC in data 2 febbraio 2012 (Prot. INGV 2052 del 27/2/2012), alle attività previste nell'ambito del Sistema Nazionale di Protezione Civile. In particolare, questo documento[1] ha finalità informative circa le osservazioni e i dati acquisiti dalle Reti di monitoraggio e osservative gestite dall'INGV. L'INGV fornisce informazioni scientifiche utilizzando le migliori conoscenze scientifiche disponibili al momento della stesura dei documenti prodotti; tuttavia, in conseguenza della complessità dei fenomeni naturali in oggetto, nulla può essere imputato all'INGV circa l'eventuale incompletezza ed incertezza dei dati riportati.
L'INGV non è responsabile dell'utilizzo, anche parziale, dei contenuti di questo documento da parte di terzi e di eventuali danni arrecati a terzi derivanti dal suo utilizzo. La proprietà dei dati contenuti in questo documento è dell'INGV.
Lo studio presentato ha beneficiato del contributo finanziario della Presidenza del Consiglio dei Ministri - Dipartimento della Protezione Civile; la presente pubblicazione, tuttavia, non riflette necessariamente la posizione e le politiche ufficiali del Dipartimento.

[1]This document is level 3 as defined in the "Principi della politica dei dati dell'INGV (D.P. n. 200 del 26.04.2016)"

GENERAL INFORMATION

Authors	Institutions	Contacts [email]	Compiling date [DD/MM/YY]
Di Giulio Giuseppe	INGV	giuseppe.digiulio@ingv.it	03/12/2021

Station description

Station name	Network code	Latitude [WGS84]	Longitude [WGS84]	Sensor depth [m]
CPC	IT	44.921	11.876	

Site characterization summary

Indicators					
fo +/ std [Hz]	Value	0,43	Quality index Qi1	0,67	
	References	see the report			
	URL of report				
Velocity profiles [YES/NO]	Value	YES	Quality index Qi1	1	
	References				
	URL of report				
Vs30 +/ std [m/s]	Value	175	Quality index Qi1	1	
	References				
	URL of report				
Surface geology [short description]	Value	Clays and silty clays	Quality index Qi1	1	
	References	see the report			
	URL of report				
Seismological bedrock depth +/ std [m]	Value	317	Quality index Qi1	0,67	
	References				
	URL of report				
Site class EC8	Value	D	Quality index Qi1	1	
	References				
	URL of report				
Engineering bedrock depth +/ std [m]	Value	317	Quality index Qi1	1	
	References				
	URL of report				

Distance from the seismic station [m]		Final quality index (Final_QI)	Comments
min	min		
15	170	0.84	QI2=0.88 , QI3=0.8

RESONANCE FREQUENCY

fo +/ STD [Hz]	0,43 +/- 0.15
Quality index 1	0,67

Source	Earthquake		Ambient noise	✔

Ambient noise

Method	H/V	✔	Ellipticity	✔	Other	
fo +/ std [Hz]	0.43		0.43			

Experiment date [DD/MM/YY]	Distance from station [m]	Lat. [WGS84]	Lon. [WGS84]
17/06/2021	15	44.921415	11.875428

Environment

Weather conditions	Sunny	Windy	Rain
	✔		
Soil sensor coupling	**Earth**	**Asphalt**	**Artificial**
	✔		
Urbanization	**None**	**Dense**	**Scattered**
			✔

Equipment

Sensor	Type [acc/vel]	manufacturer	cut off frequency [Hz]
	vel	Lennartz	0.2
Digitizer	**Type**	**Manufacturer**	**Sampling frequency [Hz]**
	130	Reftek	250
Measurement	**Number**	**Duration [min]**	
	12	180	

Analysis

Software	geopsy
Smoothing type (e.g. triangular, Konno Ohmachi, ...)	**Window length [s]**
K-O	60

Fo uncertainty estimate from

Fo from individual windows	H/V curve width	Manual picking
✔	✔	✔

Earthquake

Method	HVSR		SSR		GIT		Other	
fo +/ std [Hz]								

Recording period [DD/MM/YY]		Number of earthquakes
from	to	

Epicentral distance [km]		Magnitude range	
from	to	from	to

HVSR

Seismic phase	P	S	Coda	S + coda	All

window duration [s]	Min	Max

SSR

Seismic phase	P	S	Coda	S + coda	All

Reference station	Lat. (WGS84)	Lon. (WGS84)

window duration [s]	Min	Max

GIT

Parameters	Free (to be inverted)	Imposed
Reference paper		

Reference station	Lat. (WGS84)	Lon (WGS84)

Contacts: Cecile.Cornou@univ grenoble alpes.fr Giovanna.Cultrera@ingv.it Giuseppe.Digulio@ingv.it

Vs30

Vs30 +/ STD [m/s]	175
Quality index 1	1

Source	Geophysical measurements	✔	Geotechnical measurements		Digital Elevation Model (DEM)		Geology		DEM & Geology	

Geophysical measurements

Method	Surface waves methods (active, passive methods)		Borehole methods (DH, CH, PS Logging)	
Vs30 +/ STD [m/s]	From Vs(z)	✔	From Down Hole	
	From Vr40		From Cross Hole	
	From Vsz Vs30 correlation		From PS Logging	
Reference relationship Vsz Vs30				

Geotechnical measurements

Method	N SPT		CPT		Shear strength		OTHER	
Vs30 +/ STD [m/s]								

Experiment date [DD/MM/YY]	Distance from station [m]	Lat. [WGS84]	Lon. [WGS84]

Reference relationship Vs30 geotechnical parameter	
	N-SPT
	CPT
	Shear strength
	Other

Geology

Method	Geological map		Stratigraphic log	
Vs30 +/ STD [m/s]				
Geological map scale				
Geological unit name				
Stratigraphic log	Experiment date [DD/MM/YY]		Lat. [WGS84]	Lon. [WGS84]
Reference relationship Vs30 geology				
Reference relationship Vs30 Stratigraphic log				

Digital Elevation Model

Vs30 +/ STD [m/s]				
DEM resolution		Slope range (degree)	from	
			to	
Reference relationship Slope Vs30				

DEM & Geology

Vs30 +/ STD [m/s]	
Reference relationship Slope Vs30 geology	

Contacts: Cecile.Cornou@univ grenoble alpes.fr Giovanna.Cultrera@ingv.it Giuseppe.Digulio@ingv.it

Vs profile

Quality index 1	1

Source

Non invasive methods (active and/or passive seismics)			
Active surface waves		Refraction	
Passive surface waves	✔	Refection	
HV / ellipticity	✔		

Invasive methods (measurement in borehole)	
Cross-hole / Down-hole	
Geotechnical methods (CPT, SPT, ...)	
PS-Logging	

Non invasive : surface waves methods

Experiment date [DD/MM/YY]	Distance from station [m]		Lat. [WGS84] center location	Lon. [WGS84] center location
	Min	Max		
17/06/2021	15	170	44.921349	11.874158

Active surface waves acquisition layout

Minimum receiver spacing (m)	
Profile length (m)*	
Geophones number	
Number of profiles	

** Provide the length for the various profiles (e.g. 46 m, 94 m)*

Geophone cut-off frequency (Hz)	
Geophone type (vertical / horizontal)	
Geophone manufacturer	
Source (hammer, vibrator, ...)	
Digitizer type	
Digitizer manufacturer	

Weather conditions	Sunny	Windy	Rain	Soil sensor coupling	Earth	Asphalt	Artificial	Urbanization	None	Dense	Scattered

Passive surface waves acquisition layout

Number of sensors	> 12
Minimum array aperture	50
Maximum array aperture	200
Number of arrays	3
Minimum duration [min]	120

Sensor cut-off frequency (Hz)	0.2
Sensor type (vertical / horizontal)	geophones+Le3d5s+Terrabot 4.5 Hz
Sensor manufacturer	Geospace + Lennartz+Sara
Digitizer type	Geode+Reftek130+Terrabot
Digitizer manufacturer	Geometrics+Reftek+Sara

Weather conditions	Sunny	Windy	Rain	Soil sensor coupling	Earth	Asphalt	Artificial	Urbanization	None	Dense	Scattered
	✔				✔						✔

Type of dispersion and/or H/V estimates

		Reference paper (Name, Journal, DOI)
Rayleigh DC	✔	www.geopsy.org (RTBF)
Love DC	✔	www.geopsy.org (RTBF)
Ellipticity	✔	Raydec (Hobiger et al. 2009)
H/V (DFA, EHVR)		
H/V (SH)		

Dispersion curves

	Rayleigh	*Love*
Min wavelength (m)	6 (R0)	17
Max. wavelength (m)	320 (R1)	300
Min. phase vel. (m/s)	130 (R0)	156
Max. phase vel. (m/s)	450 (R1)	320
Modes (R0, L0, ...)	R0, R1	L0

H/V or Ellipticity curves

Min. frequency (Hz)	Max. frequency (Hz)
0.4	1

Inversion

Rayleigh waves		Love waves		Ellipticity curves		H/V (DFA, EHVR)		H/V (SH)		resonance frequency	
	✔		✔		✔						✔

A priori information used in inversion	seismic refraction		stratigraphic log		geotechnical information		water table depth	
						✔		

Inversion algorithm/code	dinver (geopsy code)
Reference	www.geopsy.org

Contacts: Cecile.Cornou@univ grenoble alpes.fr Giovanna.Cultrera@ingv.it Giuseppe.Digulio@ingv.it

Non invasive : body waves methods

Experiment date [DD/MM/YY]	Distance from station [m]		Lat. [WGS84] center location	Lon. [WGS84] center location
	Min	Max		

Acquisition layout

Receiver spacing (m)	
Profile length (m)*	
Geophones number	
Number of profiles	
Shot spacing (m) - reflection meas.	

Geophone cut-off frequency (Hz)	
Geophone type (vertical / horizontal)	
Geophone manufacturer	
Source (hammer, vibrator, ...)	
Digitizer type	
Digitizer manufacturer	

** Provide the length for the various profiles (e.g. 46 m, 94 m)*

Weather conditions	Sunny	Windy	Rain	Soil sensor coupling	Earth	Asphalt	Artificial	Urbanization	None	Dense	Scattered

Processing methods

		Reference paper (Name, Journal, DOI)
classical refraction		
refraction tomography		
classical reflection		
advanced method		

Invasive methods

	Down Hole	Cross Hole	PS Logging	SPT	CPT	OTHER
Borehole depth (m)						
Geophone type						
Source type						
Distance between wells						
Depth resolution (m)						
Latitude (WGS84)						
Longitude (WGS84)						
Distance from station (m)						
P-wave velocity						
S-wave velocity						

Processing methods

		Reference paper (Name, Journal, DOI) or ASTM norm
Down-Hole		
Cross-Hole		
PS-Logging		
SPT		
CPT		
OTHER		

Contacts: Cecile.Cornou@univ grenoble alpes.fr Giovanna.Cultrera@ingv.it Giuseppe.Digulio@ingv.it

Authoritative velocity profile

Note: You do not have to fill in all the columns. You can provide either single values for Vp or Vs (e.g. profiles derived from borehole measurements) or either a range for Vp and Vs (e.g. profiles derived from stochastic surface waves inversion)

Is Vs derived from Vp ?	**Yes**		**No**	✔

Top depth (m)	Bottom depth (m)	Vp (m/s)	STD Vp (m/s)	Vs (m/s)	STD Vs (m/s)	Vs range		Vp range	
						Vs min (m/s)	Vs max (m/s)	Vp min (m/s)	Vp max (m/s)
0	12,3	300		145					
12,3	32,6	627		203					
32,6	126,7	913		329					
126,7	317	964		552					
317	-	3166		797					

Contacts: Cecile.Cornou@univ grenoble alpes.fr Giovanna.Cultrera@ingv.it Giuseppe.Digulio@ingv.it

Figure with authoritative velocity profiles

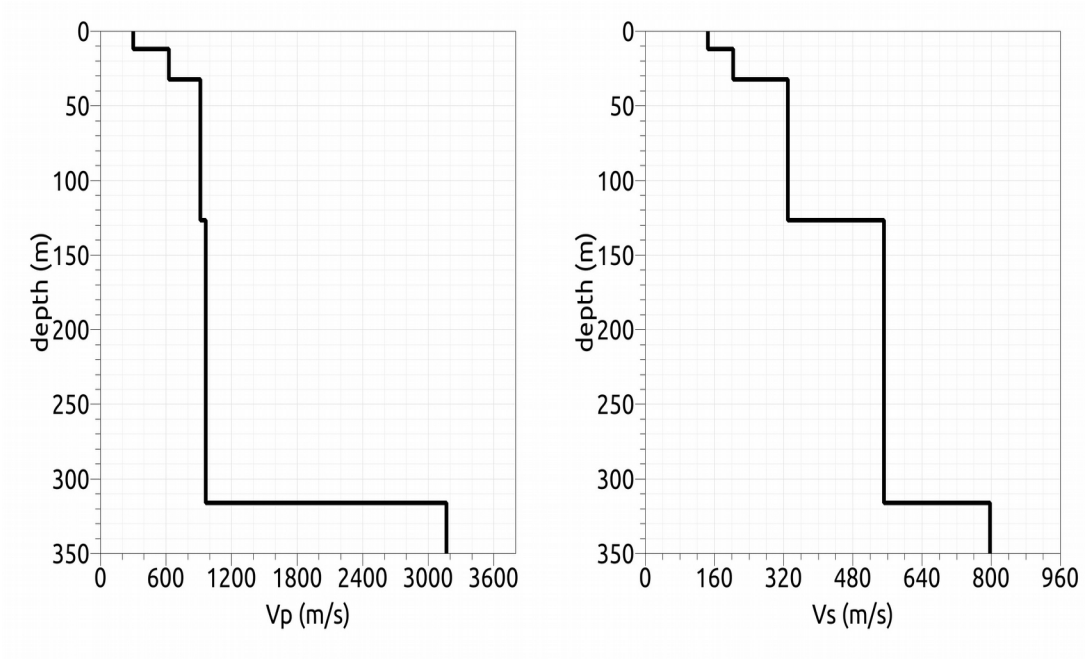

Surface geology

Quality index 1	1

Source	Cartography (geological, lithological, ...)	✔	Field survey		Stratigraphic log	✔

Geological map

Map reference	New geological map	
Map scale	1:5000	
Map sheet		
Predominent geologic/lithologic unit	Name :	AES8
	Description :	Clays and silty clays of delta Po Plain
	Age :	Holocene
	Thickness :	
	Rock mass structure :	
Fault presence		
Weathering		
Cross section		

Field survey

Map reference		
Map scale		
Predominent geologic/lithologic unit	Name :	
	Description :	
	Age :	
	Thickness :	
	Rock mass structure :	
Fault presence		
Weathering		
Cross section		

Stratigraphic log

log depth (m)	15

Top depth (m)	Bottom depth (m)	Stratigraphic description
0	13	Clays and silty clays with peat
13	15	Silty sand

Contacts: Cecile.Cornou@univ grenoble alpes.fr Giovanna.Cultrera@ingv.it Giuseppe.Digulio@ingv.it

Surface geology

Map

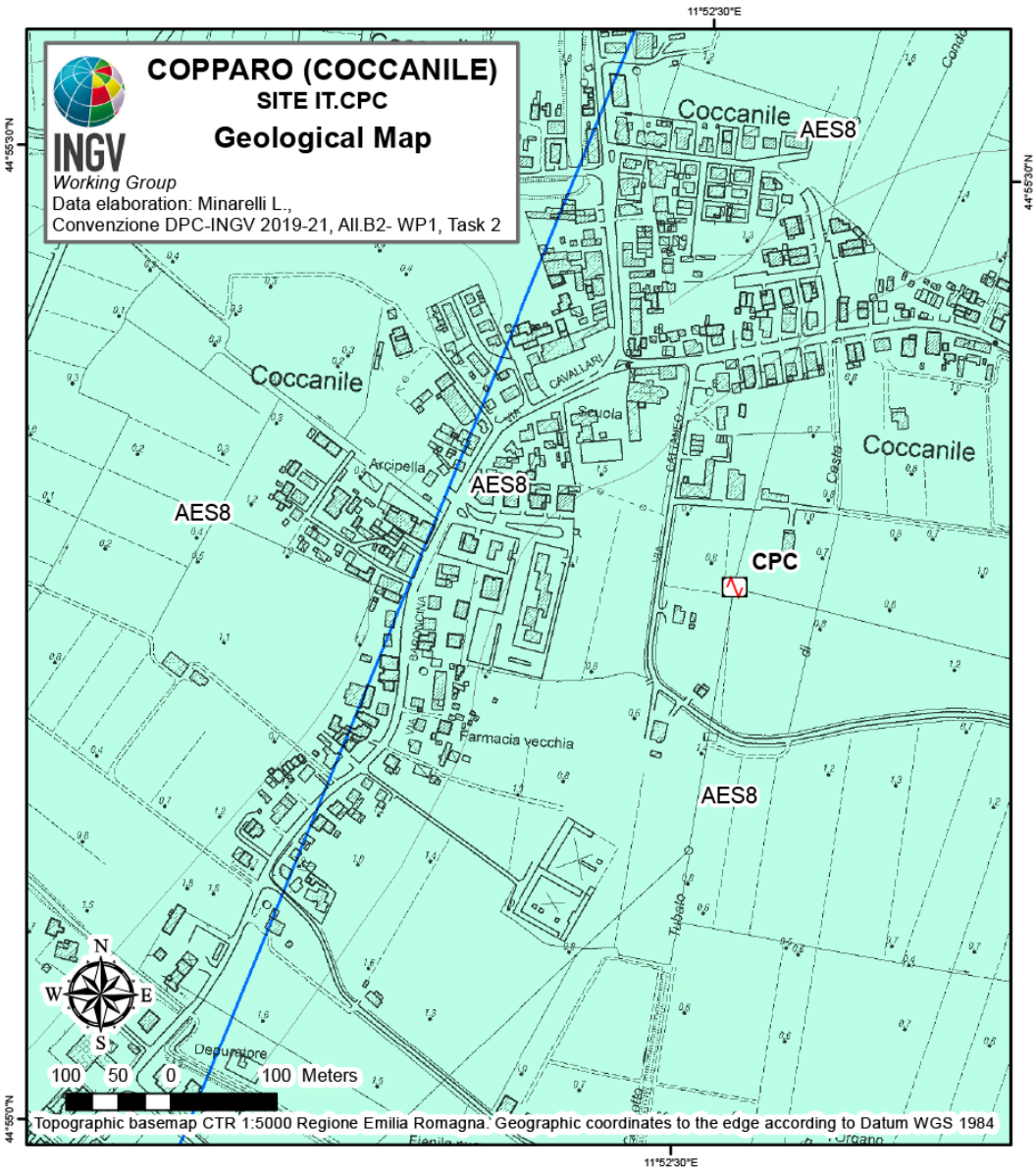

Legend

Seismic station
Stazione sismica

Traccia di sezione geologica
Trace of geological section

AES8 — Argille e argille limose di piana deltizia (Olocene)
Clays and silty clays of deltaic plain (Holocene)

AES8 — Sabbie fini limose, limi e limi argillosi di canale distributore deltizio (Olocene)
Silty sand, silt or clayey silt of deltaic distributor channel (Holocene)

Contacts: Cecile.Cornou@univ grenoble alpes.fr Giovanna.Cultrera@ingv.it Giuseppe.Digulio@ingv.it

Site class

Site class	D
Quality index 1	1

Reference building code for site classification (EC8 1, EC8 2, NEHRP, national code, ...)	EC8, NTC18

Source	Geophysical measurements	✔	Geotechnical measurements		Digital Elevation Model (DEM)		Geology		DEM & Geology	

Reference relationship geology soil class	
Reference relationship slope from DEM soil class	
Reference relationship slope from DEM geology soil class	

Parameters for deriving soil class as prescribed in building code	VS30, VSEQ

Seismological bedrock depth

Depth +/ STD [m]	317
Quality index 1	0,67

Source	Vs profiles	✔	Geology		Other (gravity, seismic refraction, TDEM, ...)	
	Resonance frequency	✔	Stratigraphic log			

Vs profile

	Non invasive methods	Invasive seismic methods	Geotechnical methods
Bedrock depth +/ STD(m)	317 +/- ?		
Bedrock Vs +/ STD(m)	317 +/- ?		
Bedrock Vp +/ STD(m)	317 +/- ?		
Is Vs derived from Vp ?	Yes		No ✔

Resonance frequency

Bedrock depth +/ STD(m)	
Reference relationship Fo bedrock depth	Rayleigh-wave ellipticity

Geology

Bedrock depth +/ STD(m)	300 +/- 20
Bedrock geological unit	AEI - Emiliano-Romagnolo Synthem
Reference	See the report

Stratigraphic log

Bedrock depth +/ STD(m)	
Bedrock geological unit	
Reference	

Other methods

	Bedrock depth +/ STD(m)	Reference
Gravity		
Seismic refraction		
Seismic reflection		
TDEM		

Contacts: Cecile.Cornou@univ grenoble alpes.fr Giovanna.Cultrera@ingv.it Giuseppe.Digulio@ingv.it

Engineering bedrock depth

Depth +/ STD [m]	317
Quality index 1	1

Reference Vs related to engineering bedrock in m/s		Reference building code for site classification (EC8 1, EC8 2, NEHRP, national code, ...)	EC8, NTC18

Source	Vs profile	✔	Geology		Stratigraphic log	

Vs profile

	Non invasive methods	Invasive seismic methods	Geotechnical methods
Bedrock depth +/ STD(m)	317 + ?		

Is Vs derived from Vp ?	Yes		No	✔

Geology

Bedrock depth +/ STD(m)	
Bedrock geological unit	
Reference	

Stratigraphic log

Bedrock depth +/ STD(m)	
Bedrock geological unit	
Reference	

Contacts: Cecile.Cornou@univ grenoble alpes.fr Giovanna.Cultrera@ingv.it Giuseppe.Digulio@ingv.it